International Journal of Applied Engineering Research ISSN 0973-4562 Volume 13, Number 19 (2018) pp. 14393-14401


# Tendon Type Robotic Gripper with Frictional Self-Locking Mechanism

**Somer Nacy 1, Wisam Abbood [2], Kostantinos Dermitzakis[3]**

*[1] Biomedical Engineering Department, University of Baghdad, Iraq.*
*[2] Automated Manufacturing Engineering Department, University of Baghdad, Iraq.*
*[3] eggze Technik GmbH, Flughofstrasse 39a, Zurich, Switzerland.*

**Abstract**

This research considers a proposed mechanism relying on frictional interactions between the grasped object and the gripper, thus attaining a case of self-locking condition for a tendon type robotic gripper. A mathematical model was derived for this proposed mechanism, upon which a special purpose apparatus was fabricated and tested. Both results, theoretically and experimentally, are in good agreement, showing that the weight of the grasped object played a major role in attaining the self-locking condition.

**Keywords:** Tendon Type Grippers, Self-locking Grippers, Frictional Locking

## INTRODUCTION

One of the main objectives of robotic manipulators is grasping objects and transfer them from place to place. The total power required to achieve this task consists of three parts, namely, the power of grasping, the power to maintain grasping and the power of transferring the object. The use of a self-locking mechanism reduces the total power by cancelling the need of the power required to maintain the grasping, in which the self-locking mechanism acts as a lock on the object to be grasped without any source of external power. A locking mechanism can function according to one of the three locking principles, namely, mechanical locking, friction-base locking, and singularity locking, Michiel et al. [1]. One of the major objectives in designing robotic grippers is providing the best conditions in the interaction between the gripper and the grasped object, which means to increase contact extension thus reaching robust and stable grasping, Lotti et al. [2].

As related to the present work, researches have been achieved on friction-base locking mechanisms as applied to robotics. Qiao et al. [3] proposed a unilateral self-locking mechanism by increasing the tractive ability of the inchworm in-pipe robots. Yong et al. [4] have developed a two-way self-locking mechanism by improving the traction ability. Fischer and Siegwart [5] designed and implemented a wheeled pole-climbing-robot based on the use of rolling self-locking mechanisms. Pulcini [6] studied the effect of different joint locking mechanisms, such as, belt brake, discrete shape and disk, on the functional performance of an under actuated robotic finger. A wheel-based cable climbing robotic system was developed by Kim et al. [7], their development was based on a special design of an adhesion mechanism which can maintain adhesion force even when the power is lost. A simulation model of mobile robot achieved by Fraczek et al. [8], this model focused on friction effects in gearing and especially on the self-locking properties. Oort et al. [9], designed and implemented an innovative knee locking mechanism for a dynamically walking robot. This mechanism is based on using a mechanical singularity to obtain an effortless lock of the knee.Joint locks for under actuated fingers were investigated by Peerdeman et al. [10], they implemented two lock concepts, namely, a gear-based concept and friction amplification mechanism. Pieterse [11] proposed two joint lock mechanisms for prosthetic fingers, these mechanisms are a gear wheel with a toothed locking pawl and friction amplifying mechanism. The frictional interaction in the tendon-pulley system of the human finger was modelled by Dermitzakis et al. [12], their results point to clear benefits of incorporating friction in tendon-driven robotic fingers for actuator mass and output forces. Dermitzakis and Carbajal [13], investigated the frictional influence in tendon-driven robotic systems. They designed a bio-inspired friction switch in which an adaptive pulley is used to minimize the influence of frictional forces under low and medium loading conditions and maximize it under high loading condition. Through this they achieved a reduction of actuator size, weight and energy consumption. A lock-based under actuated hand prosthesis was studied by Peerdeman et al. [14], they applied a series of joint locks thus serving to actively control the degrees of freedom and allowing a single actuator to perform a variety of grasping motions. Yang et al. [15] presented an innovative bilaterally controllable self-locking mechanism in which the robots tractive force is no longer restricted by the friction force. Frictional interaction has been adopted for steering low-stiffness manipulators, such as catheters, Loschak et al. [16], the proposed system suggests using a series of bead-shape vertebrae containing pull wires, these wires are tensioned to create friction between each vertebra thus preventing sliding and can steer the catheter to a desired location.

Hoeven [17] investigated a new locking mechanism, which is based on combination between a singular and a friction locking mechanisms. Kontoudis et al. [18] presented a design for the development of low-complexity, anthropomorphic, under actuated robot hands with a selectively lockable differential mechanism based on variation of the whiffle tree mechanism. Motion control of an under actuated robotic manipulator was studied by Nacy and Ibraheem [19], they implemented a locking action on the joints through electromagnetic brakes, hence to control the motion of the end effector. Chablat et al. [20] studied the change of motion modes of reconfigurable parallel robots by passing constraint singularities thus locking and releasing some passive joints of

the robot. A novel mechanism that locks a flat belt using frictional force was proposed by Shirafuji et al. [21], this mechanism was based on the folding back of the flat belt and on the change of the contact region through the use of constrained rollers. A novel mechatronic design of a robotic gripper to achieve firm and robust grasps was proposed by Hsu et al. [22], their design composed a smart self-locking under actuated mechanism to be triggered automatically when the desired grasp is achieved. Manzoor et al. [23], developed a four legged robot with self-locking mechanism, where this self-locking mechanism imparts inherent mechanical stability to the quadruped with minimum sensory equipment during motion. Kinematics, workspace and singularity analysis of a reconfigurable parallel robot was investigated by Chablat et al. [20], their study comprises a locking and unlocking of some passive joints of the robot by passing through constraint singularities.

In the present work, a simple inexpensive and light weight self-locking mechanism is proposed. It is mainly based on inducing a self-locking condition produced from a frictional force due to an elastic deformation. The model of this mechanism was derived and tested experimentally thus to validate the self-locking condition.

## THE PROPOSED MECHANISM

The tendon type robotic manipulator implemented in this study is a 1 DOF gripper, for which the CAD drawings are presented in figure 1. It consists of two links, link 1 is fixed at a known angle with respect to the horizontal, this angle is adjusted by a 12V DC self-locking worm gear servomotor and measured by the encoder supplied with it. Link 2 rotates by means of a flexible rope of 2.8mm diameter and two pulleys mechanism, where pulley 1 is attached to a 6V DC motor and pulley 2 is attached to link 2. A rotary encoder with a resolution of 500 CPR is fastened at the joint between link 1 and link 2 thus to measure the relative angular rotation.

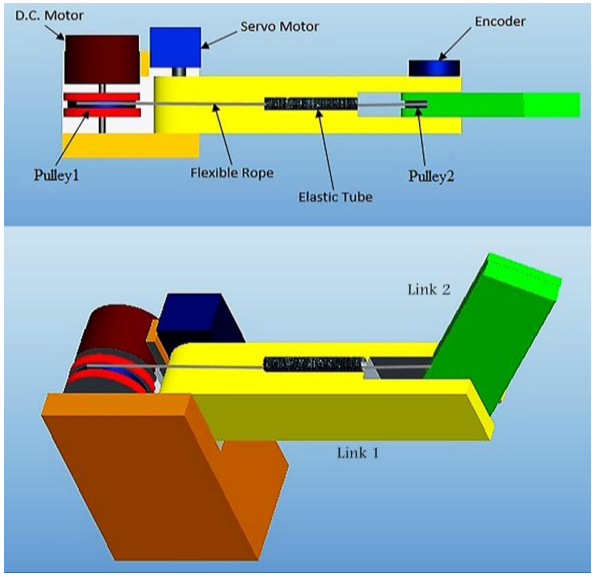


**Figure 1.** CAD drawing of the 1 DOF gripper

A schematic diagram of the gripper is shown in figure 2, showing the fixed link BO (link 1) which can be tilted with a predefined angle Ø and fixed about point O. The grasped object C is of a cylindrical shape, two different sizes were considered in this study, namely, 58mm and 34.8mm outside diameter. The flexible rope passes in an elastic tube which is adhered to link BO (link2). Two different elastic tubes were used, their specifications are shown in table1.

**Table 1.** Elastic tubes specification

| Tube No. | Material | Outside Diameter (mm) | Wall Thickness (mm) | Length (mm) | Diametral Stiffness N/mm.mm |
|---|---|---|---|---|---|
| 1 | PVC | 5.5 mm | 0.5 mm | 55 mm | 0.33443 |
| 2 | Polyester | 5 mm | 0.4 mm | 55 mm | 0.09922 |

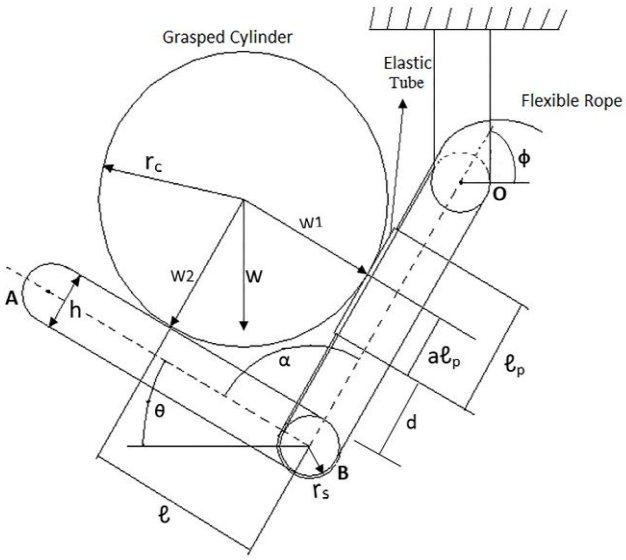


**Figure 2.** Schematic diagram of the gripper

This proposed self-locking mechanism functions on the bases of attaining a condition at which the frictional force induced between the flexible rope and the elastic tube is capable of maintaining link AB to be kept in touch with the grasped cylinder, thus grasping it without the need of any external power from the DC motor. Dimensions of this proposed gripper are shown in figure3. According to these dimensions the minimum angle between the two links is limited to 60o and the range of diameter of the grasped object is between 6.2 mm and 69.6 mm.

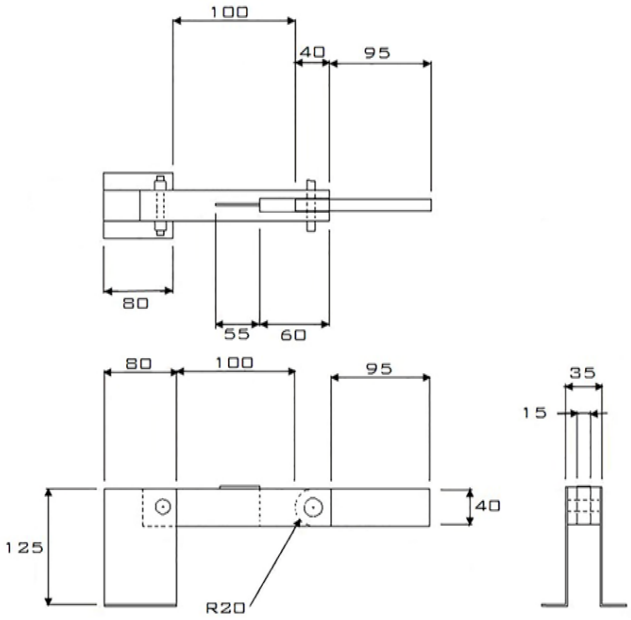


**Figure 3.** Dimensions of the gripper
(all dimension are in mm)

## MATHEMATICAL MODEL

The main purpose of deriving the mathematical model is to obtain the critical tilt angle of link 1 with respect to the horizontal (Øc), above which grasping is lost. The assumptions adopted through the analysis can be stated as follows,

1. The grasped cylindrical object undergoes no deformation during loading.
2. No extension in the flexible rope.
3. Friction is ignored at the joints and pulleys.
4. Deformation of the elastic tube is purely elastic.

The analysis is carried out by considering a state of equilibrium. Referring to figure 4, in which a state of equilibrium of the grasped cylindrical object is considered, hence

$$\sum fx = 0 \tag{1}$$

$$\sum fy = 0 \tag{2}$$

Hence, one can arrive to the following,

$$[c]\begin{bmatrix} w1 \\ w2 \end{bmatrix} = \begin{bmatrix} 0 \\ w \end{bmatrix} \tag{3}$$

Where,

$$[c] = \begin{bmatrix} \mu c\cos\phi - \sin\phi & \sin\theta \\ \mu c\sin\phi + \cos\phi & \cos\theta \end{bmatrix} \tag{4}$$

Equation (3) can be written as,

$$\begin{bmatrix} w1 \\ w2 \end{bmatrix} = c^{-1}\begin{bmatrix} 0 \\ w \end{bmatrix} \tag{5}$$

Where,

W: weight of the grasped object.

Ø: tilt angle of link 1.

θ: rotation of link 2.

μc: coefficient of friction between the grasped object and the elastic tube.

Now, it is requited to investigate the equilibrium of the gripper, which is more related to the self-locking condition. Referring to figure 5, it can be seen that there exist two torques affecting on the pulley at joint B, one is due to the grasped weight component W2 which is responsible for the extension of the gripper, while the other, under the assumption of no external tension is applied to the flexible rope, is due to the frictional force induced between the flexible rope and the elastic tube, which is due to the grasped weight component W1. Hence to achieve the self-locking condition, the following should be true,

$$\mu p \times w1 \times rs \geq w2 \times \ell \tag{6}$$

Where,

μp: coefficient of friction between the flexible rope and the elastic tube.

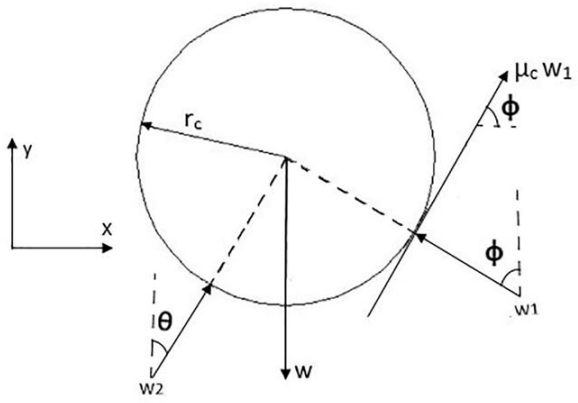


**Figure 4.** Forces on grasped cylinder

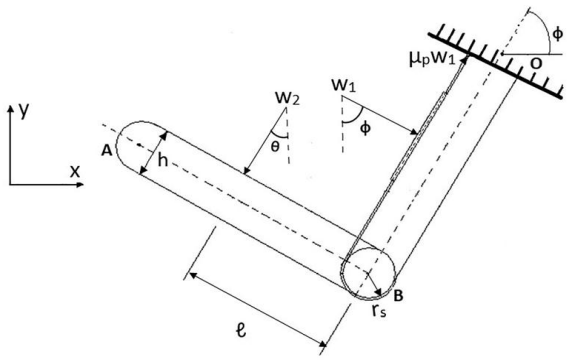


**Figure 5.** Forces on the gripper

Substituting for W1 and W2, which can be obtained from equation (5), rearranging terms to obtain,

$$\mu p \geq \frac{\ell}{rs}\left(\frac{\sin\phi - \mu c\cos\phi}{\sin\theta}\right) \quad (7)$$

## COEFFICIENTS OF FRICTION

A schematic diagram clarifying the state of contact occurring in this proposed mechanism is shown in figure 6.

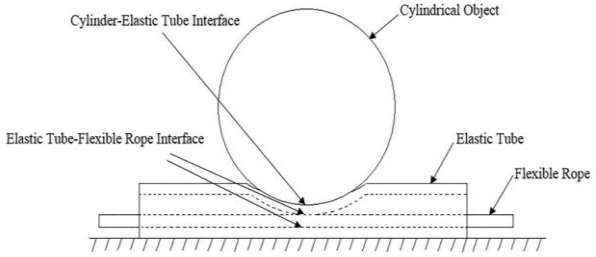


**Figure 6.** Contact between the rigid cylinder and the elastic tube

It can be seen that, there exists two regions of contact, the first is between the rigid cylinder and the elastic tube, while the second is between the elastic tube and the flexible rope sliding inside. According to previous literature, Cohen et al.[24], Popov [25], Maegawa et al. [26] and Fortunato et al.[27], friction in such a case of sliding with elastic deformation is dependent on many factors which can be summarized as follows,

- True area of contact.
- The saturation of this true area of contact.
- Non-linear viscoelasticity.
- The way in which the material around the contacting regions is sheared.
- Stick-slip sliding.

All of the above reasons give rise to a non-linear relation between the coefficient of friction with the normal applied load. Due to this complexity, experimentations were carried out to predict an empirical relation between the coefficient of friction with the normal applied load. A special purpose apparatus, as shown schematically in figure7, was designed and fabricated to carry out this task. It consists of a lever base, upon which the elastic tube is bonded, and three bolt and nut combinations, one for tilting lever base, two are attached to springs for load application on the cylindrical object and the flexible rope. All the bolts used were 10 mm in diameter and 1 mm pitch. The stiffness of the springs was 9.81 N/mm.

Two main sets of experiments were conducted, the first was to obtain the coefficient of friction between the cylindrical object and the elastic tube as related to the normal load. While the second was to obtain the coefficient of friction at the flexible rope-elastic tube interface as related to the normal load. In the first set, spring 1 is unloaded while spring 2 is loaded thus applying a normal load on the cylindrical object, then the screw to the right is turned thus lifting the free end of the lever until motion is initiated between the cylindrical object and the elastic tube, the tangent of the tilt angle of the lever indicates the coefficient of friction between the cylindrical object and the elastic tube. In the second set, the lever base is kept horizontal. Spring2 is loaded, then load is applied gradually on the flexible rope by spring 1, until the initiation of sliding of the flexible rope inside the elastic tube. The force applied by spring 2 indicates the normal force while the force applied by spring 1 indicates the friction force required to initiate sliding, from which the coefficient of friction between the flexible rope and the elastic tube can be predicted.

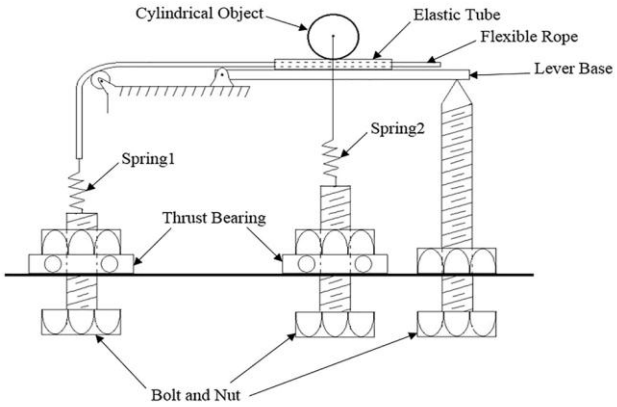


**Figure 7.** Schematic diagram of the friction measurement apparatus

Sample of results showing the relation of the coefficient of friction with the normal load are present in figures 8 and 9.

From all the results obtained and following up a best fit procedure it can be observed that the coefficient of friction between the flexible rope and the elastic tube (μp) as related to the normal load (Wn), follows the Michaelis-Menten model,

$$\mu p = \frac{A1 \times W_n}{B1 + W_n} \quad (8)$$

Where,

A1 and B1: constants

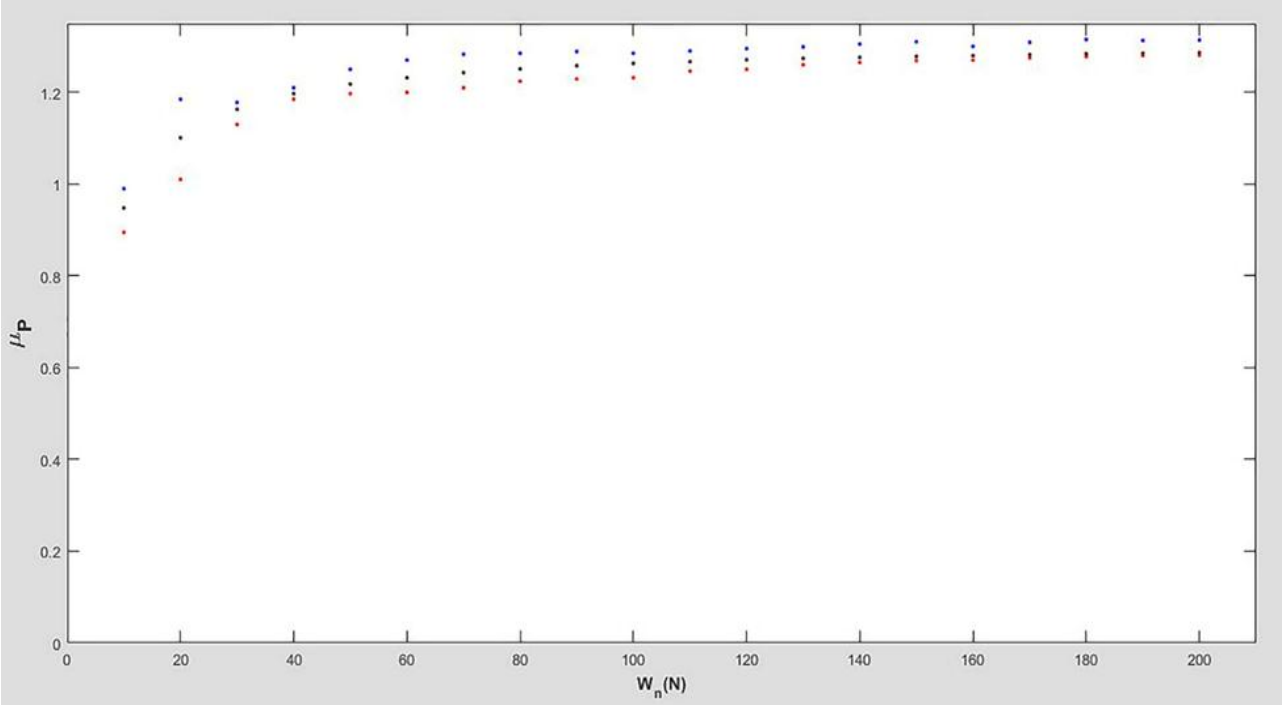


**Figure 8.** Variation of μp with normal load (Polyester elastic tube, cylinder diameter= 58mm)

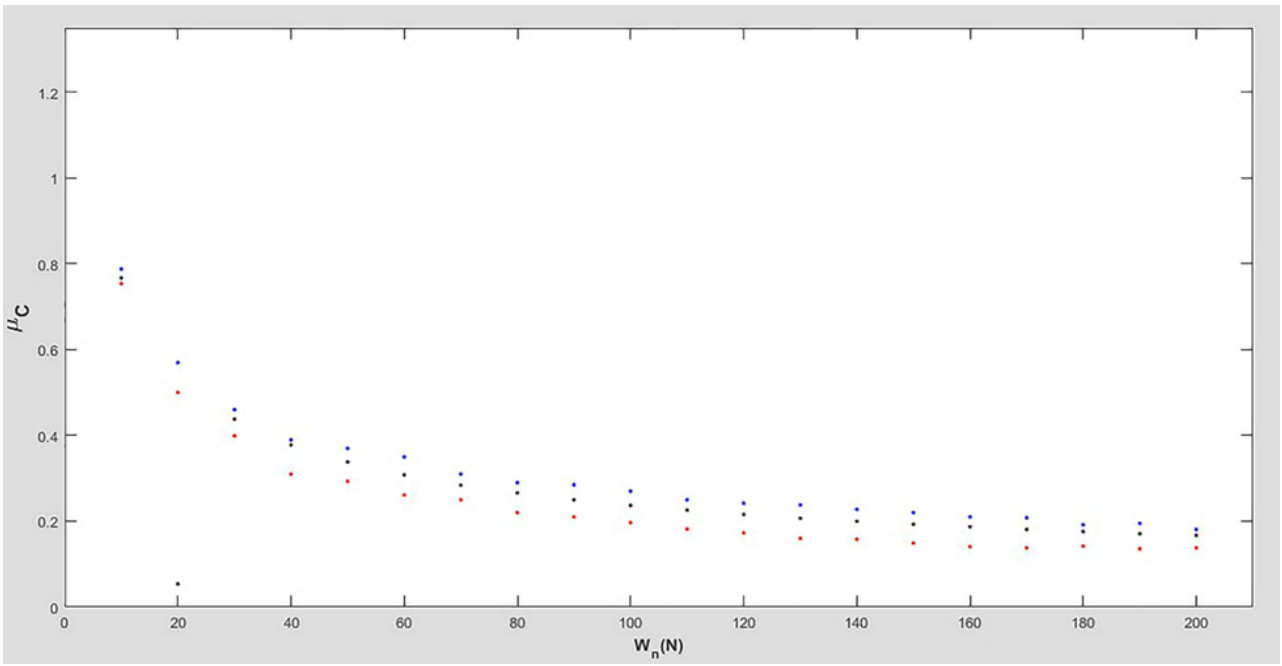


**Figure 9.** Variation of μc with normal load (PVC elastic tube, cylinder diameter= 34.8mm)

While, the relation between the coefficient of friction at the cylindrical object-elastic tube interface (μc) and the normal load obeys the power law equation,

$$\mu c = C1 \times W_n^{D1} \quad (9)$$

Where,

C1 and D1: constants

Values of the constants A1, B1, C1 and D1 for each case taken into consideration, are listed in table 2.

It is clear from the above relations that, as Wn approaches ∞, μp becomes constant approaching the value of A1 and μc approaches zero as the constant D1 is negative.

**Table 2.** Values of the constants A1, B1, C1and D1

| Type of elastic tube | Cylinder diameter (mm) | A1 | B1 | C1 | D1 | R2 Correlation coefficient for μp | R2 Correlation coefficient for μc |
|---|---|---|---|---|---|---|---|
| Polyester | 58 | 1.311 | 3.8246 | 0.7759 | -0.2334 | 98.92% | 98.53% |
| | 34.8 | 1.5319 | 6.007 | 0.6157 | -0.1825 | 99.89% | 97.99% |
| PVC | 58 | 4.5727 | 115.2552 | 2.4191 | -0.4607 | 98.78% | 98.92% |
| | 34.8 | 3.2928 | 63.8675 | 2.4833 | -0.51 | 98.91% | 99.21% |

## EXPERIMENTATION AND PROCEDURE

Experimentations were carried out to verify the performance of the proposed mechanism, thus attaining a state of self-locking without the need of any external power source. Tests were conducted by placing the cylindrical object on link 1, while it is still in a horizontal position, thus touching the elastic tube. After which power is supplied to the DC motor which in turn pulls the flexible rope thus rotating link 2 until touching the cylindrical object then the DC motor is switched off, specific load is applied to the cylindrical object thus pressing on the elastic tube. The next step is to start rotating link1 until motion initiates between the cylindrical object and link1, this motion initiation is recorded by the encoder fixed at the joint between link1 and link2. The angle of rotation of link 1 at which motion initiates is recorded by the encoder supplied with the servomotor, it is considered as the critical angle Øc at which grasping due to self-locking fails to maintain its condition. This test is repeated for different loads on the cylindrical object, hence for each applied load there exists a critical angle above which the self-locking condition is no more satisfied. For each specific load the test was repeated 5 times and the average value of Øc was obtained.

## RESULTS AND DISCUSSION

It was observed both theoretically and experimentally that for each load of the grasped object, there exists a critical tilt angle Øc above which grasping is lost or in other words, the frictional self-locking condition will no longer exist. Results of this critical angle as related to the load applied on the grasped object for the cases taken into consideration in this study, are shown in figures 10 to 13. According to the definition of stability adopted in this study, which declares that stable grasping is achieved with the existence of the frictional self-locking condition, hence values of Øc represent the border between the stable and unstable regions.

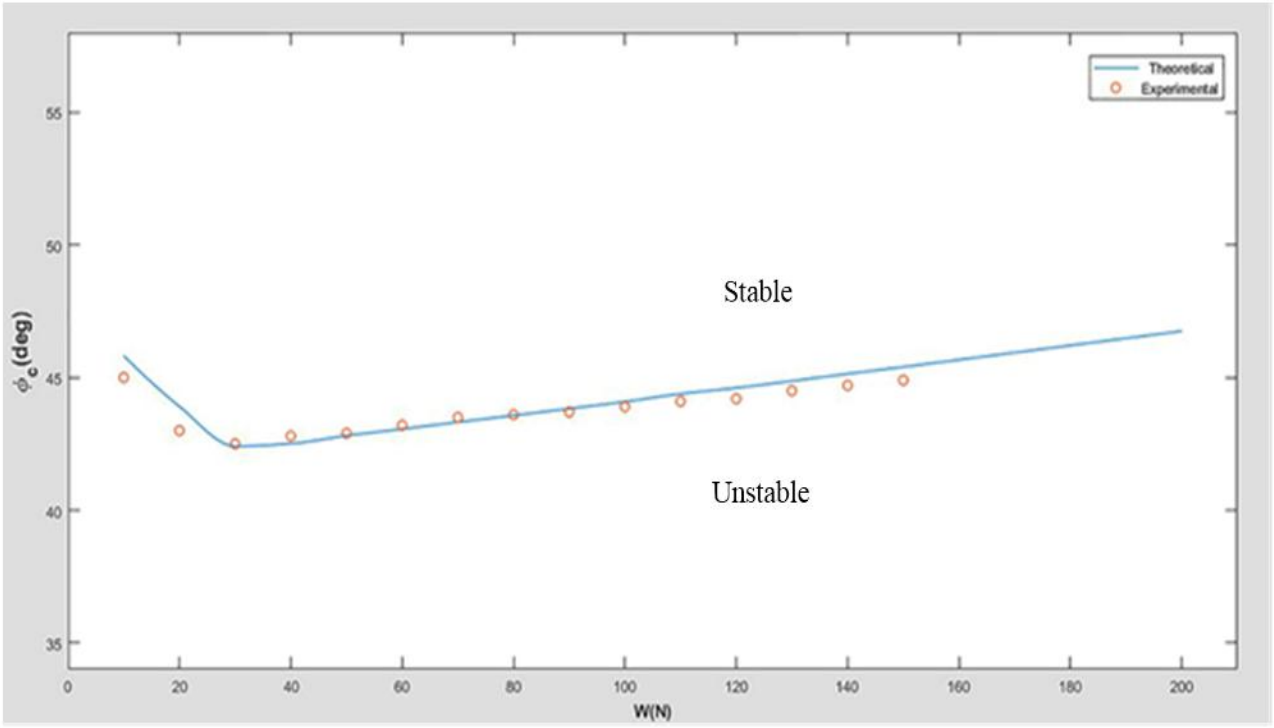


**Figure 10.** Variation of critical tilt angle with load (Polyester tube, cylinder diameter=34.8mm)

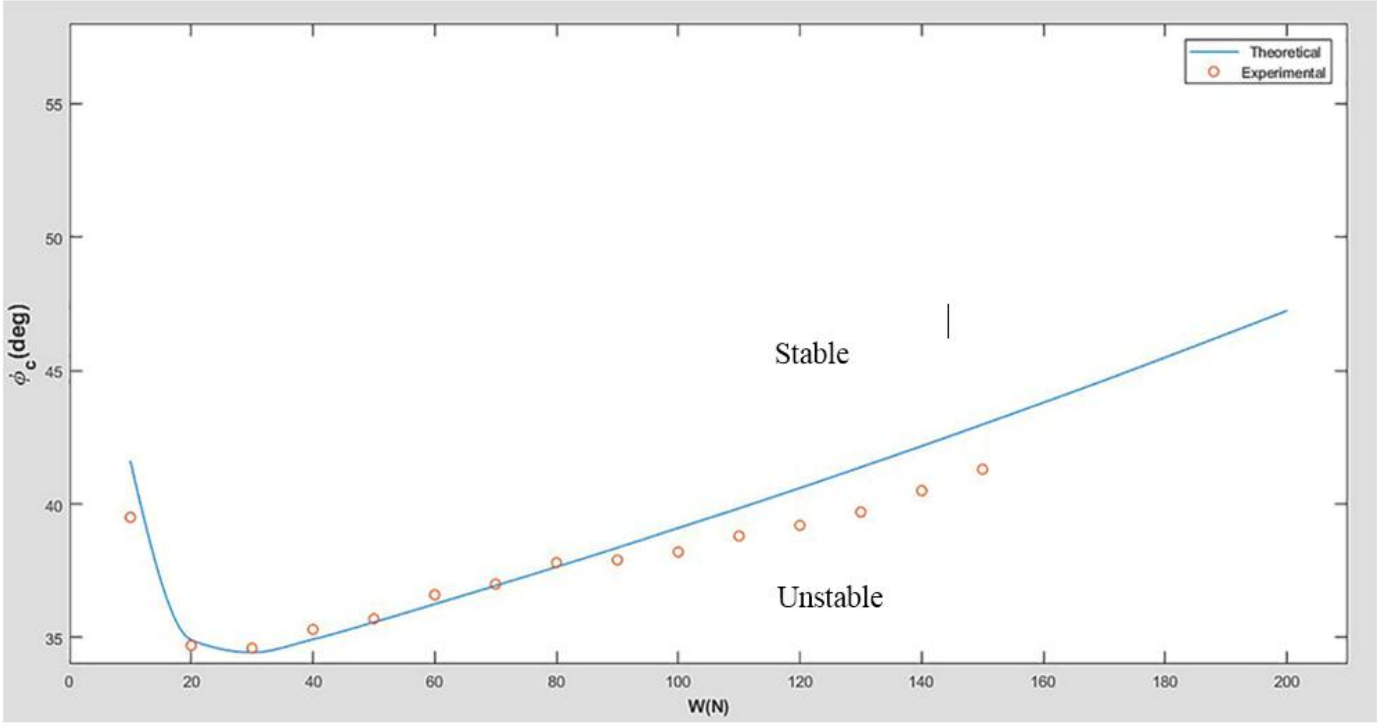


**Figure11.** Variation of critical tilt angle with load (Polyester tube, cylinder diameter=58mm)

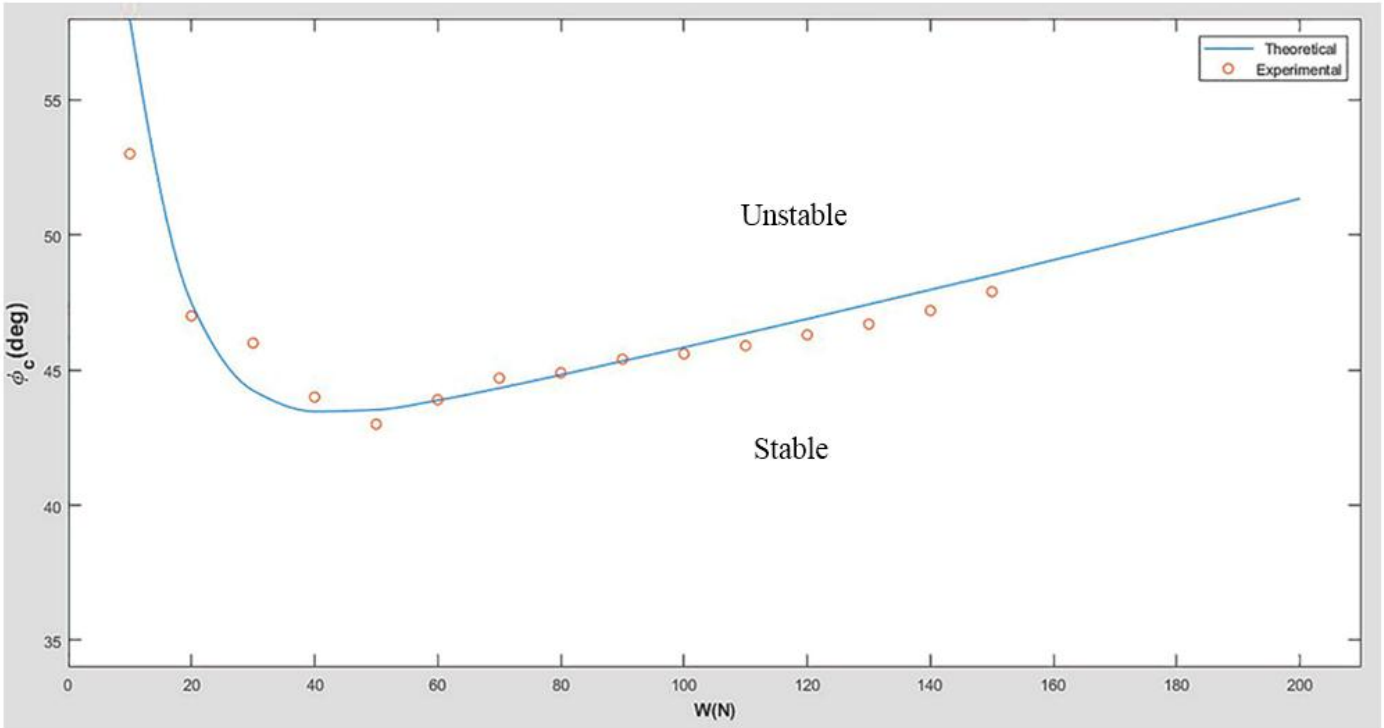


**Figure12.** Variation of critical tilt angle with load (PVC tube, cylinder diameter=34.8mm)

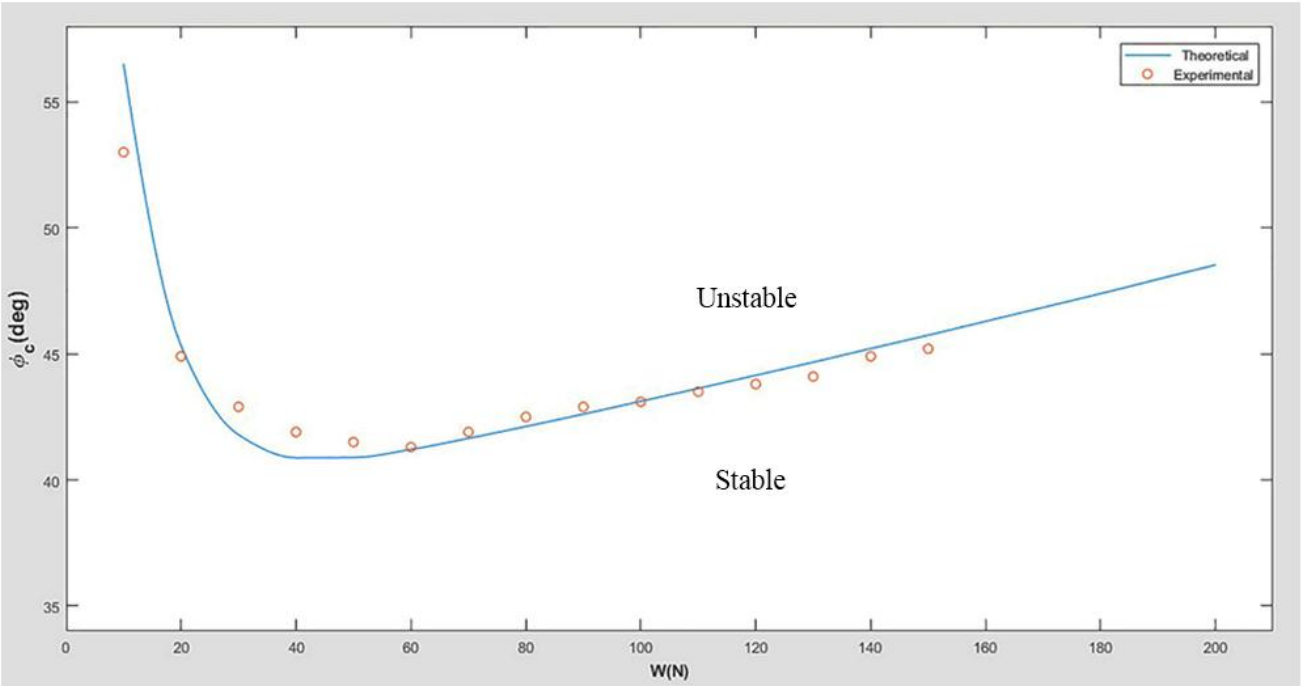


**Figure 13.** Variation of critical tilt angle with load (PVC tube, cylinder diameter=58 mm)

As a general trend the critical angle decreases initially with increasing the applied load on the grasped object until reaching a specific minimum value, after which it increases gradually. From the mathematical model, derived previously, it is clear that the tilt angle Ø is an effective factor on the self-locking condition. One other observation should be taken into account, which is related to the coefficients of friction, once at the grasped cylinder-elastic tube interface (µc), and the other at the flexible rope-elastic tube interface (µp). It can be seen that µc decreases as the load on the cylinder increases, while µp increases as the load on the cylinder increases. The contribution of these coefficients of friction in the self-locking condition produces a minima for the critical tilt angle Øc as the applied load increases.

Another observation can be withdrawn from the results is the dependence of the critical tilt angle on the size of the cylindrical grasped object, where Øc seems to be higher for cylindrical objects of smaller size, thus producing a more stable self-locking condition. This can be attributed to the higher indentation depth produced by small size cylinders as compared to larger size cylinders under identical loading condition.

## CONCLUSION

According to the results obtained, the following concluding remarks can be stated,

1. The existence of the self-locking condition for the proposed gripper.
2. A critical tilt angle was observed, above which the self-locking condition is lost thus yielding a state of unstable grasping.
3. The self-locking condition depends mainly on the size and weight of the grasped object and on the friction behavior between the mating surfaces.

## REFERENCES

[1] Plooij, M., Mathijssen, G., Cherelle, P., Lefeber, D., & Vanderborght, B., 2015, "Lock your robot: A review of locking devices in robotics," IEEE Robotics & Automation Magazine, 22(1), pp. 106-117.

[2] Lotti, F., Tiezzi, P., Vassura, G., & Zucchelli, A., 2002, "Mechanical structures for robotic hands based on the compliant mechanism concept," In 7th ESA Workshop on Advanced Space Technologies for Robotics and Automation, pp. 1-8.

[3] Qiao, J. W., Shang, J. Z., Chen, X., Luo, Z. R., & Zhang, X. P., 2010, "Unilateral self-locking mechanism for inchworm in-pipe robot," Journal of Central South University of Technology, 17(5), pp. 1043-1048.

[4] Yong, X., Jian-Zhong, S., Zi-Rong, L., Jin-Wei, Q., & Chen, C., 2010, "Development of controllable two-way self-locking mechanism for micro in-pipe robot," In International Conference on Intelligent Robotics and Applications, Springer, Berlin, Heidelberg, pp. 499-508.

[5] SIEGWART R., Fischer W., 2010, "Wheeled Pole-Climbing-Robot with High Payload Capability, Using a

Clamping Mechanism which is Inspired by the Rope-Clamps in Human Climbing," In Emerging Trends in Mobile Robotics, pp. 399-406.

[6] Pulcini, G., 2010, "Design of a miniaturized joint lock for an under actuated robotic finger," Master's thesis, University of Twente, control laboratory, Enschede.

[7] Kim, H. M., Cho, K. H., Liu, F., & Choi, H., 2011, "Development of cable climbing robotic system for inspection of suspension bridge," In International Symposium on Automation and Robotics in Construction, pp. 1422-1423.

[8] Frączek, J., Surowiec, M., & Wojtyra, M., 2011, "A simulation study of a mobile robot with self-locking speed reducers," In Multibody Dynamics 2011.

[9] Van Oort, G., Carloni, R., Borgerink, D. J., & Stramigioli, S., 2011, "An energy efficient knee locking mechanism for a dynamically walking robot," In Robotics and Automation (ICRA), 2011 IEEE International Conference on, pp. 2003-2008.

[10] Peerdeman, B., Pieterse, G. J., Stramigioli, S., Rietman, H., Hekman, E., Brouwer, D., & Misra, S., 2012, "Design of joint locks for underactuated fingers," In Biomedical Robotics and Biomechatronics (BioRob), 2012 4th IEEE RAS & EMBS International Conference on, pp. 488-493.

[11] Pieterse, G., J., 2012, "Design of a joint lock for prosthetic fingers," Master's thesis, University of Twente, engineering technology.

[12] Dermitzakis, K., Morales, M. R., & Schweizer, A., 2013, "Modeling the frictional interaction in the tendon-pulley system of the human finger for use in robotics," Artificial life, 19(1), pp. 149-169.

[13] Dermitzakis, K., & Carbajal, J. P., 2013, "Bio-inspired friction switches: adaptive pulley systems." In Intelligent Robots and Systems (IROS), 2013 IEEE/RSJ International Conference on, pp. 947-952.

[14] Peerdeman, B., Valori, M., Brouwer, D., Hekman, E., Misra, S., & Stramigioli, S., 2014, "UT hand I: A lock-based underactuated hand prosthesis," Mechanism and machine theory, 78, pp. 307-323.

[15] Yong, X., Jian-Zhong, S., Zi-Rong, L., Jin-Wei, Q., & Chen, C., 2010, "Development of controllable two-way self-locking mechanism for micro in-pipe robot," In International Conference on Intelligent Robotics and Applications, Springer, Berlin, Heidelberg, pp. 499-508.

[16] Loschak, P. M., Burke, S. F., Zumbro, E., Forelli, A. R., & Howe, R. D., 2015, "A robotic system for actively stiffening flexible manipulators," In Intelligent Robots and Systems (IROS), 2015 IEEE/RSJ International Conference on, pp. 216-221.

[17] Van der Hoeven, T. R. M., 2015, "Statically balanced singular-friction locking," Master's thesis, Delft University of Technology, Mechanical, Maritime and Materials Engineering, BioMechanical Engineering.

[18] Kontoudis, G. P., Liarokapis, M. V., Zisimatos, A. G., Mavrogiannis, C. I., & Kyriakopoulos, K. J., 2015, "Open-source, anthropomorphic, underactuated robot hands with a selectively lockable differential mechanism: Towards affordable prostheses," In Intelligent Robots and Systems (IROS), 2015 IEEE/RSJ International Conference on, pp. 5857-5862.

[19] Nacy, S., M., &Ibraheem, S., T., 2016, "Motion Control of an Underactuated 2-DOF Robotic Manipulator," Control theory and informatics, 6(3), pp.74-82.

[20] Chablat, D., Kong, X., & Zhang, C., 2017, "Kinematics, workspace and singularity analysis of a multi-mode parallel robot," In ASME 2017 International Design Engineering Technical Conferences and Computers and Information in Engineering Conference, pp. V05AT08A040-V05AT08A040.

[21] Shirafuji, S., Matsui, N., & Ota, J., 2017, "Novel frictional-locking-mechanism for a flat belt: Theory, mechanism, and validation," Mechanism and Machine Theory, 116, pp. 371-382.

[22] Hsu, J., Yoshida, E., Harada, K., & Kheddar, A., 2017, "Self-locking underactuated mechanism for robotic gripper," In Advanced Intelligent Mechatronics (AIM), 2017 IEEE International Conference on, pp. 620-627.

[23] Manzoor, M. T., Sohail, U., Nizami, M. H. A., & Ayaz, Y., 2017, "Design of a Single Motor Based Leg Structure with the Consideration of Inherent Mechanical Stability," In IOP Conference Series: Materials Science and Engineering, 224(1), p. 012041.

[24] Cohen, D., Kligerman, Y., & Etsion, I., 2008, "A model for contact and static friction of nominally flat rough surfaces under full stick contact condition," Journal of Tribology, 130(3), p. 031401.

[25] Popov, V. L., 2010, "Contact mechanics and friction," Berlin: Springer Berlin Heidelberg.

[26] Maegawa, S., Itoigawa, F., & Nakamura, T., 2015, "Effect of normal load on friction coefficient for sliding contact between rough rubber surface and rigid smooth plane," Tribology International, 92, pp. 335-343.

[27] Fortunato, G., Ciaravola, V., Furno, A., Scaraggi, M., Lorenz, B., & Persson, B. N., 2017, "Dependency of rubber friction on normal force or load: theory and experiment," Tire Science and Technology, 45(1), pp. 25-54.